WIENER-HOPF ANALYSIS OF PLANAR CANONICAL STRUCTURES LOADED WITH LONGITUDINALLY MAGNETIZED PLASMA BIASED NORMALLY TO THE EXTRAORDINARY WAVE PROPAGATION

G. A. Kyriacou

Department of Electrical and Computer Engineering
Democritus University of Thrace
12 Vas. Sofias Str., Xanthi, GR-67100, Greece

Abstract—The canonical problem of an extra-ordinary Transverse Electromagnetic wave propagating in a parallel plane waveguide with a semi-infinite upper conductor and loaded with magnetized plasma is considered. The homogeneous biasing constant magnetic field is assumed parallel to the substrate and normal to the wave propagation, which incidents normally on the truncated edge. The Wiener-Hopf technique is employed and the corresponding equations are formulated for the open-radiating structure as well as for a closed one resulting from the placement of a metallic shield parallel to the waveguide planes. Closed form field expressions are obtained for the shielded geometry, while the open geometry Kernel factorization is left for future extensions. Important non-reciprocal wave propagation phenomena are involved, which lend non-even function properties to the involved Kernels. Hence, their factorization becomes non-trivial requiring new mathematical approaches. Finally, a review of the involved non-reciprocal and/or unidirectional surface waves is given, which is related to the involved mathematical complexities.

1. INTRODUCTION

When ferrite or plasma materials are subject to constant magnetic field they exhibit anisotropic permeability ($\overline{\overline{\mu}}_r$) and permittivity ($\overline{\overline{\varepsilon}}_r$) respectively. These tensor constitutive parameters depend on both the biasing magnetic field and the operating frequency, e.g., [1–3]. This dependence enables their dynamic control through the DC current of an electromagnet, which generates the biasing constant magnetic field. These exceptional features offered by ferrites are extensively used

in microwave waveguide, stripline and microstrip devices from long ago. In particular their non-reciprocal field propagation characteristics are unique and make these materials indispensable in microwave applications. Recently, the exploitation of these features in printed antenna applications received a considerable research effort, e.g., [2, 4–7]. These include wideband electronic frequency tuning, beam steering and possible surface wave and RCS reduction.

In contrary to the above there was only a limited use of magnetized ion gas plasmas in microwave devices. In antenna applications there was a considerable research effort mainly because these antennas were embedded in a magnetized plasma in their operating environment, as for example in satellite communications and nuclear fusion, e.g., [8–10]. However, there was only a minor effort in the direction of exploiting the magnetized plasma features in printed antennas, e.g., [11, 12, 32–35]. This lack may due to the difficulties in generating and controlling ionized gas plasma. Besides, the evolution in the electronic solid state plasma technology may enable its application in integrated microwave devices and printed antennas. High quality semiconductors in terms of purity and crystallographic perfection are known to behave as "solid state plasma" at cryogenic temperatures (liquid nitrogen, about 77°K) as early as 1970 and before that, e.g., Hoyaux [32]. Their practical exploitation is postponed until recently that cryogenic technology advancement made the operation of these devices attainable. High quality n-type doped GaAs substrate seems to be a very good candidate for the implementation of non-reciprocal microwave devices as isolators, phase shifters and circulators in integrated circuit form. Working toward this aim Bolle and his colleagues [33, 34], studied a GaAs substrate magnetized parallel to its surface but normal to the wave direction of propagation. They assumed n-type GaAs with carrier concentration $N = 2.1 \times 10^{15}$ electrons/cm^3 equivalent to a plasma frequency $\omega_p = 10^{13}$ rad/sec and a DC magnetic field $B_0 = 3810$ Gauss yielding a cyclotron frequency $\omega_c = 10^{12}$ rad/sec. These data are appropriate for the modeling of quasi optical non-reciprocal devices. Likewise, Ivanov and Nikolaev [35] studied the same structure but with the DC-biasing magnetic field aligned parallel to the propagation direction. Besides these works, the magnetized plasma slab or sheath, either free or grounded at the one surface, was extensively studied in the 1960 decade, e.g., Seshadri and his colleagues [26], Ishimaru [29] and Johansen [21]. Even though these works did not refer to solid-state plasma, the permittivity tensor is identically the same and the theory developed is exactly applicable. Some recently published studies [11, 13–15] based on numerical techniques are directed toward printed antenna applications.

The present effort aims at the solution of a canonical problem of a TEM wave propagating in a parallel-plane waveguide with a semi-infinite upper conductor loaded with a magnetized plasma and normally incident on the edge defined by the truncated upper conductor (Fig. 1). The Wiener-Hopf technique is employed for the estimation of the scattered field at the edge and consequently the reflected TEM wave propagating back, in the parallel plane region. The reflection coefficient to be established can be used in the study of a patch antenna based on the transverse resonance technique, according to our previous work [16]. This approach is based on the approximation that a TEM wave (possibly emanating from a probe feed) propagating zig-zag in the parallel plane region below a rectangular patch radiator incidents almost normally on its radiating edge. This was actually observed for any rectangular patch radiator operating at its dominant mode. Besides, independently from the above described specific application the solution of the canonical problem (scattering from the edge of the truncated conductor) is by itself a significant contribution. A lot of interesting phenomena regarding the excitation of surface waves in the grounded plasma region and the radiated space wave can be explained through the scattered field expressions. The dependence of the turn-on/off conditions from the plasma parameters and especially the magnetizing DC field are of particular importance. Moreover, unique non-reciprocal phenomena in the propagation of surface waves on grounded plasma slabs have been revealed by Ishimaru [29] and Seshadri, e.g., [26]. Concerning the application of the Wiener-Hopf technique in parallel plane anisotropic structures, some related work has been carried out by Kobayashi et al. [27, 28], who studied the dielectric/ferrite loading case. The present effort will try to contribute to the understanding of these waves' excitation and their field distributions. Additionally, higher order modes of this grounded structure are expected to become leaky waves in the same manner as in isotropic printed structures. These may also offer non-reciprocal features in their radiation mechanisms. All these type of modes will be involved in the final inverse Fourier Transform required for the evaluation of the near and far field of the structure. Even though leaky waves study constitutes a research challenge, it cannot be included in the present paper, but it would be reserved for future efforts. Note that there isn't yet any published work on such non-reciprocal leaky waves.

One possible question could be raised at this point as "why do you try analyzing magnetized plasma since extensively studied magnetized ferrites offer the same features"? This is not exactly true, because the magnetized plasma ($\overline{\overline{\varepsilon}}_r$) behaves as the dual of magnetized ferrites

$(\overline{\overline{\mu}}_r)$. So plasma may be more suitable for some applications than ferrite material and vice-versa. For example, in a parallel plane loaded with ferrite the dominant TEM mode is the ordinary one (which is unaffected from the biasing-controlling DC bias), since the extraordinary TEM mode has an electric field component parallel to the two metallic planes. In contrary, in the magnetized plasma case this occurs vice-versa and the tuneable extra-ordinary TEM mode becomes dominant. From this observation one may conclude that is more convenient to exploit the dynamic $\overline{\overline{\varepsilon}}_r$ control in patch antennas printed-placed on magnetized (solid state) plasma.

Besides, the "open-radiating" structure applications, the proposed canonical problem solution may serve the study of numerous important closed-shielded printed structures. First, field scattering from the open end of microstrip lines printed on plasma substrate is very important in the design of microwave devices. Second, considering the ferrite experience, important non-reciprocal devices lend their operation to edge-guided modes.

Summarizing the above, this paper will be restricted to the theoretical solution of the canonical problem referring to the edge scattering for normal incidence of an extra-ordinary TEM wave. The theoretical Wiener-Hopf formulation for both the shielded and open structure will be given, but only the exact solution of the shielded geometry will be finished. The solutions for the open-structure based on a limiting approach where the shield distance tends to infinity; will be left for a follow-up work. Namely, the present work tries to put the bases for numerous challenging research topics.

2. FORMULATION OF THE CANONICAL PROBLEM

2.1. Definition of the Canonical Problem

The geometry to be studied is shown in Fig. 1. Basically it consists of a parallel plane waveguide loaded with magnetized plasma, where the lower conductor (ground plane) and the plasma substrate are assumed extending to infinity while a semi-infinite (truncated, $z < 0$) upper conductor is considered. The biasing constant magnetic field ($\overline{H}_{dc}$) is assumed parallel to the two planes and parallel to the edge ($\hat{y}$-axis, $\overline{H}_{dc} = H_O \widehat{y}$) of the truncated plane conductor.

The extra-ordinary TEM wave (possibly emanating from a probe feed) propagating in the parallel plane region along the $\hat{z}$-axis (transverse to $\overline{H}_{dc}$) is considered to be incident normally on the edge defined by the truncated upper conductor.
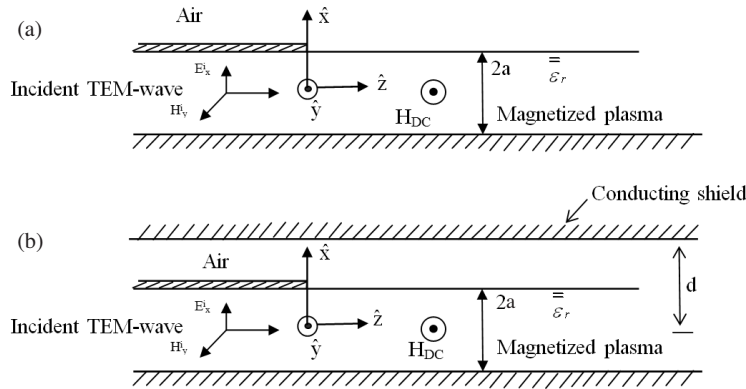
Figure 1. A TEM wave incident upon the edge defined by the truncate upper conductor of a parallel plane waveguide loaded with longitudinally magnetized plasma: (a) open and (b) Shielded structure. Wave propagation normal to the biasing DC magnetic field is considered.

2.2. Fourier Transform in the Direction Normal to the Edge

Time harmonic fields $(e^{j\omega t})$ and a spatial (z-axis) to a λ-space (propagation constants) spectrum Fourier transform pair is considered (in the form $e^{j\kappa_0\lambda\cdot z}$) as follows:

$$\tilde{f}(\lambda) = \frac{\kappa_0}{2\pi}\left\{\int_{-\infty}^{0} + \int_{0}^{\infty}\right\} f(z)e^{j\kappa_0\lambda\cdot z}dz = \tilde{f}_-(\lambda) + \tilde{f}_+(\lambda) \qquad (1)$$

and

$$f_+(z) = \begin{cases} \int_{C_+} \tilde{f}_+(\lambda)e^{-j\kappa_0\lambda\cdot z}d\lambda & \text{for } z \geq 0 \\ 0 & \text{for } z < 0 \end{cases} \qquad (2a)$$

$$f_-(z) = \begin{cases} \int_{C_-} \tilde{f}_-(\lambda)e^{-j\kappa_0\lambda\cdot z}d\lambda & \text{for } z \leq 0 \\ 0 & \text{for } z > 0 \end{cases} \qquad (2b)$$

The spectral functions $\tilde{f}_-(\lambda)$ and $\tilde{f}_+(\lambda)$ are analytic in the lower and upper λ half-planes respectively, hence are also called "negative" and "positive" functions. On the other hand the spatial functions $f_+(z)$ and $f_-(z)$ are defined only in the positive and negative z half-planes

respectively or:

$$f(z) = f_-(z) + f_+(z) \qquad (2c)$$

As shown in Fig. 2 the contour C_+ must be closed in the lower λ half-plane when $f_+(z)$ for $z > 0$ will be recovered employing Cauchy's formula. Note that closing C_+ in the upper λ half-plane, where $\tilde{f}_+(\lambda)$ is analytic, ensures that $f_+(z)$ is identically zero for $z < 0$. Likewise, when $f_-(z)$ for $z < 0$ is to be recovered, then the integration contour C_- must be closed in the upper λ half-plane.
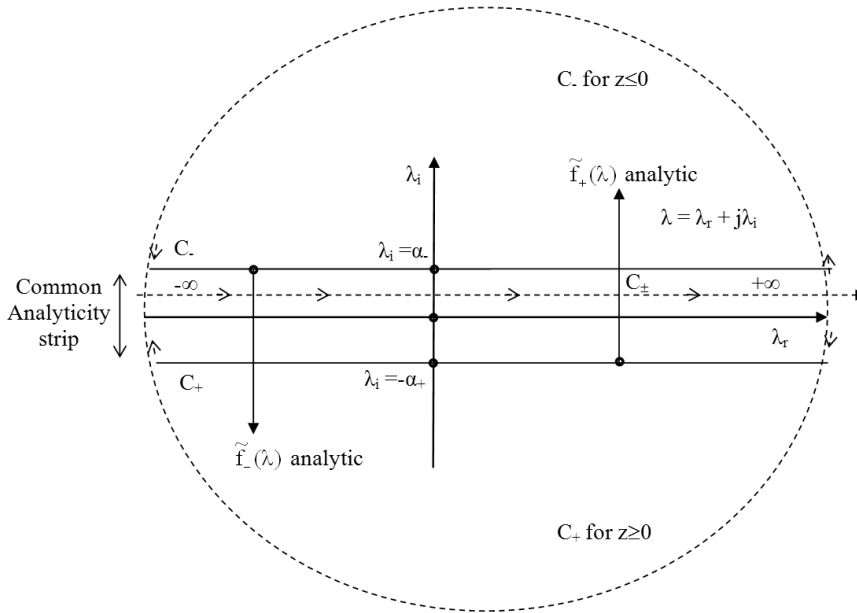

Figure 2. Definitions of $\tilde{f}_+(\lambda)$ and $\tilde{f}_-(\lambda)$ analyticity regions and the appropriate C_+, C_- integration contours.

Note that this selection of contours ensures that the integrands will tend to zero at infinity ($|z| \to \infty$) or equivalently that the associated field expressions will obey the radiation condition at infinity (assuming the presence of at least small losses). Also, note that the above definitions may be encountered in the literature, e.g., Collin [25, p.826], denoted in the opposite sense. This is due to the opposite signs in the Fourier transform pair considered therein.

2.3. Simplifications to Maxwell Equations

The basic derivative property of Fourier transforms results in a simplification of the wave equation by substituting $\partial/\partial z = -j\kappa_0\lambda$. This consequence is the same as when propagation along the z-axis like $e^{-j\kappa_0\lambda z}$ is assumed. Since the excited extra-ordinary TEM wave propagating in the parallel plane region ($z < 0$) is assumed to be incident normally on the edge $z = 0$, there will be no variation of the scattered field in the also infinitely extending y-direction. This in turn results to a further simplification of $\partial/\partial y = 0$. Moreover, the magnetized plasma ($\overline{H}_{DC} = H_0\hat{y}$) relative permittivity tensor is also given in [21] as:

$$\overline{\overline{\varepsilon}}_r = \begin{bmatrix} \varepsilon_{r1} & 0 & j\varepsilon_{r2} \\ 0 & \varepsilon_{r3} & 0 \\ -j\varepsilon_{r2} & 0 & \varepsilon_{r1} \end{bmatrix} \tag{3a}$$

where

$$\varepsilon_{r1} = \frac{\Omega^2 - R^2 - 1}{\Omega^2 - R^2}, \quad \varepsilon_{r2} = \frac{R}{\Omega(\Omega^2 - R^2)}, \quad \varepsilon_{r3} = 1 - \frac{1}{\Omega^2} \tag{3b}$$

and

$$\Omega = \omega/\omega_p, \quad R = \omega_c/\omega_p, \quad \omega_p^2 = Ne^2/m\varepsilon_0 = \gamma \cdot Ne/\varepsilon_0,$$
$$\omega_c = -e\mu_0 \mathrm{H}_0/m = -\gamma\mu_0 \mathrm{H}_0 \tag{3c}$$

The plasma frequency is symbolized as ω_p and its gyromagnetic frequency as ω_c. Also, e and m are the charge and the mass of an electron, $\gamma = e/m$ is the magneto-mechanic or gyromagnetic ratio (gyroelectric ratio could be more appropriate for magnetized plasmas) and ε_0, μ_0 are the free space permittivity and permeability. Also, N is the average density of electrons.

   Regarding the Wiener-Hopf formulation the Jones method is employed for convenience reasons, [22, 23]. Namely, the wave equation solution and the application of the boundary conditions are carried out in the transformed λ-domain.

2.4. General Solutions of the Wave Equations

With the above considerations, the wave equation for the scattered magnetic field in the transformed λ-domain ($\tilde{H}_y^s$) and for the plasma region $-a \leq x \leq a$ can be written as:

$$\left[\frac{\partial^2}{\partial x^2} + \kappa_0^2 \left(\frac{\varepsilon_{rq}}{\varepsilon_{r1}} - \lambda^2 \right) \right] \tilde{H}_y^s = 0 \tag{4}$$

where $\kappa_0 = \omega\sqrt{\mu_0\varepsilon_0}$ the free space wavenumber, $\varepsilon_{rq} = \varepsilon_{r1}^2 - \varepsilon_{r2}^2$ and the transverse effective permittivity is $\varepsilon_{r_{eff}} = \varepsilon_{rq}/\varepsilon_{r1}$.

The general solution of (4) in the plasma region $-a \leq x \leq a$ takes the form:

$$\tilde{H}_y^s = B_p(\lambda)\cosh(\kappa_0 u_p x) + C_p(\lambda)\sinh(\kappa_0 u_p x) \quad \text{for} -a \leq x \leq a \quad (5a)$$

where

$$u_p = \sqrt{\lambda^2 - \varepsilon_{r_{eff}}^2} = \sqrt{\lambda^2 - \varepsilon_{rq}/\varepsilon_{r1}} \quad \text{and} \quad \text{Re}(u_p) \geq 0. \quad (5b)$$

The transverse field components can also be expressed in the transformed domain by just expanding the Maxwell rotational equations and using the above simplifications:

$$\tilde{E}_x^s = \frac{\zeta_0}{\varepsilon_{rq}}\left\{\lambda\varepsilon_{r1}\tilde{H}_y^s - \frac{\varepsilon_{r2}}{\kappa_0}\frac{\partial\tilde{H}_y^s}{\partial x}\right\} \quad (6a)$$

$$\tilde{E}_z^s = j\frac{\zeta_0}{\varepsilon_{rq}}\left\{\lambda\varepsilon_{r2}\tilde{H}_y^s - \frac{\varepsilon_{r1}}{\kappa_0}\frac{\partial\tilde{H}_y^s}{\partial x}\right\} \quad (6b)$$

where $\zeta_0 = \sqrt{\mu_0/\varepsilon_0} = 120\pi\,\Omega$ the free space characteristic impedance.

Substituting the general solution (5) into (6) the transverse components in the plasma region $(-a \leq x \leq a)$ read:

$$
\begin{aligned}
\tilde{E}_x^s &= \frac{\zeta_0}{\varepsilon_{rq}}\left\{[\lambda\cdot\varepsilon_{r1}\cdot B_p(\lambda) - \varepsilon_{r2}\cdot u_p\cdot C_p(\lambda)]\cosh(\kappa_0 u_p x)\right\} \\
&\quad + [\lambda\cdot\varepsilon_{r1}\cdot C_p(\lambda) - \varepsilon_{r2}\cdot u_p\cdot B_p(\lambda)]\sinh(\kappa_0 u_p x) \\
&= \frac{\zeta_0}{\varepsilon_{rq}}[A_{xc}(\lambda)\cdot\cosh(\kappa_0 u_p x) + A_{xs}(\lambda)\cdot\sinh(\kappa_0 u_p x)] \quad (7a)
\end{aligned}
$$

$$
\begin{aligned}
\tilde{E}_z^s &= j\frac{\zeta_0}{\varepsilon_{rq}}\left\{[\lambda\cdot\varepsilon_{r2}\cdot B_p(\lambda) - \varepsilon_{r1}\cdot u_p\cdot C_p(\lambda)]\cosh(\kappa_0 u_p x)\right\} \\
&\quad + [\lambda\cdot\varepsilon_{r2}\cdot C_p(\lambda) - \varepsilon_{r1}\cdot u_p\cdot B_p(\lambda)]\sinh(\kappa_0 u_p x) \\
&= j\frac{\zeta_0}{\varepsilon_{rq}}[A_{zc}(\lambda)\cdot\cosh(\kappa_0 u_p x) + A_{zs}(\lambda)\cdot\sinh(\kappa_0 u_p x)] \quad (7b)
\end{aligned}
$$

It is interesting as well as useful for the further analysis to see how the electric flux density components $\tilde{\vec{D}} = \bar{\bar{\varepsilon}}\cdot\tilde{\vec{E}}$ are simplified when Equations (6) are exploited. Namely, using (3a) their definition yields:

$$\tilde{D}_x^s = \varepsilon_0\left(\varepsilon_{r1}\tilde{E}_x^s + j\varepsilon_{r2}\tilde{E}_z^s\right) = \zeta_0\varepsilon_0\lambda\tilde{H}_y^s \quad (7c)$$

$$\tilde{D}_z^s = \varepsilon_0\left(-j\varepsilon_{r2}\tilde{E}_x^s + \varepsilon_{r1}\tilde{E}_z^s\right) = \frac{1}{j\omega}\frac{\partial\tilde{H}_y^s}{\partial x} \quad (7d)$$

The remaining field components vanish ($\tilde{E}_y^s = \tilde{H}_x^s = \tilde{H}_z^s = 0$ and $\tilde{D}_y^s = 0$) due to the assumption of the absence of propagation in the y-direction, ($\partial/\partial y = 0$).

The general solution for the air region can be obtained by substituting in Equations (4)–(7) its characteristics ($\varepsilon_{r1} = \varepsilon_{r3} = 1$, $\varepsilon_{r2} = 0$). Besides, this solution must also obey the radiation condition at infinity, so for the air region $x \geq a$, we have:

$$\tilde{H}_y^s = A_p(\lambda) \cdot e^{-\kappa_0 u_0 (x-a)} \quad \text{for} \quad x \geq a \tag{8}$$

with $u_0 = \sqrt{\lambda^2 - 1}$ and $\text{Re}(u_0) \geq 0$, and

$$\tilde{E}_x^s = -\frac{1}{j\omega\varepsilon_0} \frac{\partial \tilde{H}_y^s}{\partial z} = \zeta_0 \cdot \lambda \cdot \tilde{H}_y^s \tag{9a}$$

$$\tilde{E}_z^s = \frac{1}{j\omega\varepsilon_0} \frac{\partial \tilde{H}_y^s}{\partial x} = j\zeta_0 u_0 \cdot \tilde{H}_y^s \tag{9b}$$

Similarly, the electric flux density components are written as:

$$\tilde{D}_x^s = \varepsilon_0 \tilde{E}_x^s = \zeta_0 \varepsilon_0 \lambda \tilde{H}_y^s \tag{9c}$$

$$\tilde{D}_z^s = \varepsilon_0 \tilde{E}_z^s = \frac{1}{j\omega} \frac{\partial \tilde{H}_y}{\partial x} = j\zeta_0 \varepsilon_0 u_0 \tilde{H}_y^s \tag{9d}$$

Note that the electric flux density expressions (7c), (7d) and (9c), (9d) are formally the same in the plasma and air region. However, their difference lies on the different magnetic field expressions (5a) and (8). The quantities $A_p(\lambda)$, $B_p(\lambda)$ and $C_p(\lambda)$ involved in the above equations are arbitrary spectral functions to be estimated by enforcing the appropriate boundary conditions.

The incident extra-ordinary TEM wave propagating in the parallel-plane region toward the positive z-direction is given by Johansen, [21] as well as Mittra and Lee [36], in the spatial domain as:

$$H_y^i = \exp\left(\kappa_0 \varepsilon_{r2} x / \sqrt{\varepsilon_{r1}} - j\kappa_0 \sqrt{\varepsilon_{r1}} z\right) \tag{10}$$

and

$$E_x^i = (\zeta_0 / \sqrt{\varepsilon_{r1}}) \cdot H_y^i \tag{11}$$

where a unit amplitude is assumed for H_y^i just for convenience. Note that it is $E_z^i = 0$ as expected for a TEM wave propagating in the z-direction.

The scattering on the edge will excite a reflected TEM wave along with higher order modes. However, the latter will in turn vanish at a relatively small distance from the edge, provided that the plasma-substrate thickness is small enough, in order for these modes to be below cut-off. The reflected TEM wave propagating in the parallel plane region toward the negative z-direction can be expressed again in the spatial domain as, [21]:

$$H_y^r = \Gamma_{TEM} \cdot \exp\left(-\kappa_0 \varepsilon_{r2} \cdot x/\sqrt{\varepsilon_{r1}} + j\kappa_0\sqrt{\varepsilon_{r1}}z\right) \qquad (12a)$$

and

$$E_x^r = (-\zeta_0/\sqrt{\varepsilon_{r1}}) \cdot H_y^r \qquad (12b)$$

where Γ_{TEM} is the complex reflection coefficient to be sought from the study of the scattering at the edge, using Wiener-Hopf technique.

2.5. Inhomogeneous Boundary Conditions and Wiener-Hopf Equations

A pair of Wiener-Hopf equations can be obtained through the enforcement of the boundary conditions in the transformed λ-domain. Specifically, the scattered tangential electric field $\tilde{E}_z^s$ must vanish on the metallic ground plane $(x = -a)$ and preserve its continuity at the plasma-air interface at $x = a$. Note that the corresponding tangential component of the incident field as well as that of the dominant TEM reflected mode are identically zero $(E_z^i = E_z^r = 0)$. In turn, these requirements yield the following expressions:

$$\tilde{E}_z^s(x = -a, \lambda) = 0 \ \leftrightarrow \ A_{zc}(\lambda) = A_{zs}(\lambda) \cdot \tanh(\kappa_0 u_p a) \qquad (13a)$$

$$\tilde{E}_z^s(x = a^-, \lambda) = \tilde{E}_z^s(x = a^+, \lambda) \leftrightarrow$$
$$\leftrightarrow j\frac{\zeta_0}{\varepsilon_{rq}}\left[A_{zc}(\lambda)\cosh(\kappa_0 u_p a) + A_{zs}(\lambda)\cdot\sinh(\kappa_0 u_p a)\right] = j\zeta_0 u_0 A_p(\lambda) \quad (13b)$$

Combining Equations (13a) and (13b) yields:

$$A_{zs}(\lambda) = u_0 A_p(\lambda) \cdot (\varepsilon_{rq}/2\sinh(\kappa_0 u_p a)) \qquad (13c)$$
$$A_{zc}(\lambda) = u_0 A_p(\lambda) \cdot (\varepsilon_{rq}/2\cosh(\kappa_0 u_p a)) \qquad (13d)$$

Besides the above, the tangential electric field (in the spatial domain) must vanish on the truncated upper conductor $(x = a, z < 0)$. For

this purpose, one may consider the spectral expression (9b) through (8) and apply the inverse Fourier transform (2a) to yield:

$$E_z^s(x = a^+, z < 0) = f_+(z)|_{z<0} = j\zeta_0 \int_{c_+} u_0 A_p(\lambda) \cdot e^{-j\kappa_0\lambda z} = 0 \quad (14)$$

In order to satisfy (14), we are looking for a function which must be identically zero for $z < 0$ and with a-value $f_+(z) \neq 0$ to be defined for $z > 0$. This may result from the inverse Fourier transform of a "positive" spectral function $\tilde{R}_+(\lambda) = u_0 A_p(\lambda)$ analytic in the upper λ half-plane. Using the two previously described boundary conditions in Equations (13) and the definitions of $A_{zc}(\lambda)$ and $A_{zs}(\lambda)$ indirectly given in (7b), then the two spectral functions $B_p(\lambda)$ and $C_p(\lambda)$ are also expressed in terms of $\tilde{R}_+(\lambda)$ as follows:

$$A_p(\lambda) = \tilde{R}_+(\lambda)/u_0 \quad \leftrightarrow \quad \tilde{R}_+(\lambda) = u_0 \cdot A_p(\lambda) \quad (15a)$$

$$B_p(\lambda) = \frac{\varepsilon_{rq} \cdot \tilde{R}_+(\lambda)}{2[(\lambda\varepsilon_{r2})^2 - (\varepsilon_{r1} \cdot u_p)^2]} \cdot \left(\frac{\lambda \cdot \varepsilon_{r2}}{\cosh(\kappa_0 u_p a)} + \frac{\varepsilon_{r1} \cdot u_p}{\sinh(\kappa_0 u_p a)} \right) \quad (15b)$$

$$C_p(\lambda) = \frac{\varepsilon_{rq} \cdot \tilde{R}_+(\lambda)}{2[(\lambda\varepsilon_{r2})^2 - (\varepsilon_{r1} \cdot u_p)^2]} \cdot \left(\frac{\varepsilon_{r1} \cdot u_p}{\cosh(\kappa_0 u_p a)} + \frac{\lambda \cdot \varepsilon_{r2}}{\sinh(\kappa_0 u_p a)} \right) \quad (15c)$$

Note that the common term in (15b) and (15c) can be simplified by exploiting the definitions of the involved quantities, e.g., Equation (5b), as:

$$\frac{\varepsilon_{rq}}{2[(\lambda\varepsilon_{r2})^2 - (\varepsilon_{r1} \cdot u_p)^2]} = -\frac{1}{2(\lambda^2 - \varepsilon_{r1})} \quad (15d)$$

The dependence of the scattered field from the incident extra-ordinary TEM wave (excitation) can be obtained either by applying the continuity of the total normal electric flux density $D_{x,tot}$, or the continuity of the total tangential magnetic field $H_{y,tot}$ at the plasma-air interface ($x = a$, $z > 0$). *At this point we assume that the incident field propagates un-attenuated in the region $z > 0$, or that it exists in the area* ($|x| \leq a$, $-\infty < z < +\infty$). This is a usual assumption in the Wiener-Hopf technique, e.g., [23, p.126], since it simplifies the problem. Besides that, its contribution can be evaluated and subtracted latter on, as it is represented by the corresponding residue of the propagating field. Imposing in turn the latter boundary condition for $H_{y,tot} = H_y^s + H_y^i$ in the spatial domain, yields:

$$H_y^s(x=a^-, z>0) + H_y^i(x=a^-, z>0) = H_y^s(x=a^+, z>0) \quad \text{for} \quad z>0$$
$$(16)$$

Instead of working with the assumed incident field in the region $z > 0$ and since the above condition is applied only at the interface $x = a$, it is more convenient to introduce the associate surface current density $J^i_{sz+}(z)$. This is a fictitious current density that could be induced at the interface ($x = a$, $z > 0$) if a conductor would be placed there. Namely,

$$\hat{n}x\hat{y}H^i_y(x = a^-, z > 0)\big|_{\hat{n}=-\hat{x}} = -\hat{z}H^i_y(x = a^-, z > 0) = \hat{z}J^i_{sz+}(z) \tag{17}$$

In order to express Equation (16) in the spectral domain the above current density should be also transformed. Since this is a non-trivial function only for positive-z its transform should be a "positive" spectral function $\tilde{j}^i_+(\lambda)$ which through (10) reads:

$$\tilde{j}^i_+(\lambda) = -\frac{\kappa_0}{2\pi}\int_0^\infty H^i_y(x = a^-, z)e^{j\kappa_0\lambda z}dz = -j\frac{1}{2\pi(\lambda - \sqrt{\varepsilon_{r1}})} \cdot e^{\kappa_0\varepsilon_{r2}a/\sqrt{\varepsilon_{r1}}} \tag{18}$$

Returning back to Equation (16) and transferring all terms in the right hand side, it is obvious that this can be fulfilled by a function $f_-(z)$ which according to (2b) is identically zero for $z > 0$, as:

$$f_-(z) = H^s_y(x = a^+, z) - H^s_y(x = a^-, z) + J^i_{sz+}(z) \tag{19}$$

In turn the Fourier transform of $f_-(z)$ can be defined as a "negative" spectral function $\tilde{L}_-(\lambda)$ as:

$$\tilde{L}_-(\lambda) = \tilde{H}^s_y(x = a^+, \lambda) - \tilde{H}^s_y(x = a^-, \lambda) + \tilde{j}^i_+(\lambda) \quad \text{valid for} \quad z > 0 \tag{20}$$

Reformulating the above expressions by exploiting (17) yields a Wiener-Hopf equation of the form:

$$Q(\lambda)\tilde{R}_+(\lambda) = \tilde{L}_-(\lambda) - \tilde{j}^i_+(\lambda) \tag{21}$$

where

$$Q(\lambda) = \frac{1}{u_0} + \frac{\lambda\varepsilon_{r2} + \varepsilon_{r1} \cdot u_p \cdot \coth(2\kappa_0 u_p a)}{(\lambda^2 - \varepsilon_{r1})} \tag{22}$$

Note that the argument of the cotangent in (22) involves the full thickness of the substrate (2a) rather than the half one (a) involved in the previous expressions.

2.6. An Alternative Wiener-Hopf Equation for the Parallel Plane Region

Even though the Wiener-Hopf equation given in (21) includes all the necessary information, one may extract a similar equation for the parallel plane region $z < 0$. In this case, the current density induced on the truncated conductor $J_{sz-}^s(z)$ should be included as:

$$H_y^s(x=a^+, z<0) - H_y^s(x=a^-, z<0) - H_y^i(x=a^-, z<0) = J_{sz-}^s(z<0) \tag{23}$$

Note that the induced current density $J_{sz-}^s(z)$ exists only for $z < 0$ and is identically zero for $z > 0$. So, its Fourier transform is a "negative" spectral function $\tilde{j}_-^s(\lambda)$ according to the definition (2b). Likewise, the known incident field can be represented on the truncated conductor by an equivalent induced surface current density $J_{sz}^i(z < 0)$. In the λ-domain this will be represented by a negative function $\tilde{j}_-^i(\lambda)$ as:

$$\tilde{j}_-^i(\lambda) = -\frac{\kappa_0}{2\pi} \int\limits_{-\infty}^{0} H_y^i(x = a^-, z) e^{j\kappa_0 \lambda z} dz = +j\frac{e^{\kappa_0 \varepsilon_{r2} a/\sqrt{\varepsilon_{r1}}}}{2\pi(\lambda + \sqrt{\varepsilon_{r1}})} \tag{24}$$

Note that the main difference between (18) and (24) is a change of sign in the denominator, but this is enough to reverse their analyticity from the upper to the lower λ half-planes. Specifically, the inverse Fourier transform of $\tilde{j}_+^i(z)$ defined in (18) involves a pole at $\lambda = +\sqrt{\varepsilon_{r1}}$ located in the lower λ-half plane. In contrary, $\tilde{j}_-^i(z)$ defined in (24) involves a pole at $\lambda = -\sqrt{\varepsilon_{r1}}$ located in the upper λ-half plane. These can be clearly justified when the plasma media losses are included as $\varepsilon_{r1} = \varepsilon_{r1}'(1 - j\tan\delta_1) = \varepsilon_{r1}' e^{j\delta_1}/\cos\delta_1$.

Transferring all terms of (23) to the left hand side we may represent their sum by a function $g_+(z)$ which must be identically zero for $z < 0$. Hence, its Fourier transform should be a "positive" spectral function $\tilde{G}_+(\lambda)$ as:

$$\tilde{G}_+(\lambda) = \tilde{H}_y^s(x = a^+, \lambda) - \tilde{H}_y^s(x = a^-, \lambda) + \tilde{j}_-^i(\lambda) - \tilde{j}_-^s(\lambda) \tag{25}$$

Substituting for the field expressions, (23) yields an alternative magnetic field Wiener-Hopf equation of the form:

$$Q(\lambda) \cdot \tilde{R}_+(\lambda) = \tilde{G}_+(\lambda) - \tilde{j}_-^i(\lambda) + \tilde{j}_-^s(\lambda) \tag{26}$$

where $Q(\lambda)$ is still given by (22).

From a first point of view, Equation (26) is more complicated than (21), however the major difficulty in the solution at both equations is the factorization of $Q(\lambda)$ into a product of "positive" and "negative" functions.

2.7. Wiener-Hopf Equation for the Charge Density

The only boundary condition missing from the above consideration is the continuity of the normal electric flux density D_x. However, it is classically expected that the normal components boundary conditions do not offer any additional information when analytical methods are employed (in contrary they may be necessary within numerical approaches). Hence, the same Wiener-Hopf equation is expected. Let us consider the plasma air interface at $(x = a, z > 0)$ and once again assume the incident field propagating un-attenuated beyond the edge $z = 0$ toward $z > 0$. Then, the boundary condition for D_x reads:

$$D_x^s(x = a^+, z > 0) - D_x^s(x = a^-, z > 0) = \rho_+^i(z > 0) \qquad (27)$$

The fictitious charge density $\rho_+^i(z > 0)$ corresponds to $J_{sz+}^i(z > 0)$. Using (17) ρ_+^i and its spectral equivalent $\tilde{\rho}_+^i(\lambda)$ becomes:

$$\vec{\nabla} \cdot \vec{J}_{sz+}^i = -j\omega\rho_+^i \;\rightarrow\; \rho_+^i = -\frac{1}{j\omega}\frac{\partial J_{sz+}^i}{\partial z} \;\Leftrightarrow\; \tilde{\rho}_+^i(\lambda) = -\zeta_0\varepsilon_0\lambda\tilde{H}_y^i(x = a^-, \lambda)$$
$$(28)$$

Moreover, the normal flux density in the spectral domain $\tilde{D}_x^s$ is already expressed in terms of $\tilde{H}_y^s$ in Equation (7c) or (9c) as:

$$\tilde{D}_x^s = \zeta_0 \cdot \varepsilon_0 \cdot \lambda \cdot \tilde{H}_y^s \qquad (29)$$

In view of (28) and (29) the condition (27) leads exactly to (20), ensuring that it does not offer any additional information. Likewise, the boundary condition of D_x on the truncated conductor ($x = a$, $z < 0$) yields again (26).

It's worth noting that herein only one Wiener-Hopf equation is obtained in contrary to the general case of oblique incidence, e.g., [18, 19, 20], when a pair of these equations occurs. This is due to the assumption of normal incidence at the edge $z = 0$ and the resulting field independence from y-coordinate. Referring for example to [26] or [37], the Kernel Q involved in (21) can be symbolized as $Q \rightarrow 1/Q_e$, which is associated to the E-modes excited in the grounded plasma slab ($z > 0$, $|x| \leq a$). In turn their characteristic equation can be obtained by setting $Q = 0$.

2.8. E-modes of Grounded Plasma Slab

Usually the characteristic equation is obtained by directly applying the boundary conditions at the metallic ground plane $x = -a$ and

at the plasma-air interface $x = a$ (in the absence of any truncated upper conductor). However, any one can relatively easy prove that this is identical to enforcing Q to zero, which actually involves the same boundary conditions. The grounded plasma slab in its isotropic (unmagnetized) state was studied by Tamir and Oliner [37]. Besides, Seshadri and his collaborators devoted a series of works, e.g., [26], to its magnetized anisotropic state. In both cases two type of modes where discriminated, when excited by a corresponding $\hat{y}$-directed line source as:

E-modes or TM$_x$ (Fig. 1): (E_z, E_x, H_y) and $(H_x = H_z = E_y = 0)$ excited by an electric $\hat{y}$ line source.

H-modes or TE_x (Fig. 1): (E_y, H_x, H_z) and $(E_x = E_z = H_y = 0)$ excited by a magnetic $\hat{y}$ line source.

From the analysis of the previous sections it can be concluded that the edge along $\hat{y}$ excites only E-modes in the grounded plasma layer $z > 0$. Specifically their characteristic equation reads:

E-modes: $\leftrightarrow Q = 0$:

$$\varepsilon_{r1} \cdot u_0 \cdot u_p \cdot \coth(2\kappa_0 u_p a) + \lambda \cdot \varepsilon_{r2} \cdot u_0 + \lambda^2 - \varepsilon_{r1} = 0 \qquad (30)$$

The propagation constant (β) in the z-direction is identical to $\kappa_0 \lambda$, namely $\beta = k_0 \lambda$. In the limiting case of an isotropic substrate $\varepsilon_{r2} = 0$ Equation (30) is reduced to:

Isotropic dielectric: $\varepsilon_{r2} = 0 \rightarrow \varepsilon_{rq} = \varepsilon_{r1}^2$ and $u_p = \sqrt{\lambda^2 - \varepsilon_{r1}}$:

$$u_p \tanh(\kappa_0 u_p 2a) = -\varepsilon_{r1} \cdot u_0 \qquad (31)$$

The roots of (30), namely the surface or leaky wave propagation constants, are the zeros of Q or the poles of the Kernel $Q_e(\lambda) = 1/Q(\lambda)$. These will in turn account for the residue contributions in the inverse Fourier integral providing the scattered field in the spatial domain.

A close examination of (30) reveals an important property of the characteristic equation and the related modes which is exclusively due to the plasma anisotropy, namely to the term $(\lambda \varepsilon_{r2} u_0)$. These surface waves properties propagated on grounded magnetized plasma were extensively studied by Seshadri et al. [26] and Ishimaru [29]. Most of these studies elaborated on their unidirectional propagation characteristics, reviewed next in an abstract form. Hence, it is this property that causes difficulties in the solution of the Wiener-Hopf equation (21). A general approach for exploiting modes characteristics in complex anisotropic media is given by Barybin [38]. Specifically, the key factorization procedure of the Kernels like $Q(\lambda)$ have been devised for even functions $Q_e(\lambda) = Q_e(-\lambda)$. However, $Q(\lambda)$ defined in (22) is not an even function, exactly due to the anisotropy term $(\lambda \varepsilon_{r2} u_0)$. Since, λ represents the complex propagation constant in the x-direction, it is necessary to review their properties.

2.9. Unidirectional Forward and Backward Surface Waves

Recall that the assumed Fourier transform (1), (2) yields $\partial/\partial z = -j\kappa_0\lambda$ which is equivalent to a propagation dependence $e^{-j\kappa_0\lambda\cdot z}$. Thus, for the $e^{+j\omega t}$ time dependence the positive λ corresponds to a normalized propagation constant in the positive z-direction and vice-versa.

According to [26] the solutions of (30) can be classified into two types of surface waves as follows:

Type-1 surface waves: Existing only in the frequency range $1 < \Omega < \sqrt{1 + R^2}$.

They have a normalized cutoff frequency $\Omega = \omega/\omega_p > 1$ and they are always "forward" waves in the sense that their phase (v_p) and group (v_g) velocities have the same sign $(v_p v_g > 0)$. In the ideal case when plasma losses are negligible an infinite number of type-1 surface waves exist near the resonance $\Omega = \sqrt{1 + R^2}$ where $\varepsilon_{r1} \to 0$ or $\varepsilon_{rq} \to \infty$ and the unbounded plasma wavenumber $k = k_0\sqrt{\varepsilon_{rq}/\varepsilon_{r1}}$ becomes also infinite. However, when losses are taken into account the number of these modes is drastically reduced. But, the most interesting property for the following analysis refers to their different characteristics when they propagate in the positive or the negative z-direction.

Type-2 surface waves: Existing in the frequency range $0 < \Omega < \sqrt{1 + R^2}$.

These modes do not have a low frequency cutoff and they also have different characteristics (unequal propagation constants) when they propagate in the positive or in the negative z-direction. Usually, there is only one dispersion curve for positive wavenumbers (positive λ), but there are two dispersion curves for negative wavenumbers. Depending on the plasma slab thickness (2a) and the value of R which is controlled by the DC magnetization (see Equation (3c)), the positive and one of the negative dispersion curves may present frequency ranges with "backward" behavior. Recall that backward waves are those with different signs in the phase and group velocities $(v_p v_g < 0)$. Namely, the wave propagates in the positive z-direction (positive wavenumber) but the net energy flow occurs in the negative z-direction (opposite wavenumber and group velocity, which is always pointing along the Poynting vector).

Unidirectional surface waves: At this point it is worth noting that in the low frequency region as $\Omega \to 0$, $\varepsilon_{r2} \to -\infty$ while ε_{r1} remains finite, thus $|\varepsilon_{r2}|/\varepsilon_{r1} \to \infty$. In turn the wave has a very large attenuation in the plasma region and a relatively small attenuation in the air, in contrary to the ordinary surface waves, [26, p.537]. This causes the wave energy to be concentrated either on the top or the

bottom plasma surface resulting into unidirectional type-2 surface waves. Specifically, a wave in the plasma slab propagating in the positive $\hat{z}$ direction behaves as in Equation (8): $\propto e^{\kappa_0 \varepsilon_{r2} x / \sqrt{\varepsilon_{r1}}}$. $e^{-j\kappa_0 \sqrt{\varepsilon_{r1}} \cdot z}$ where in the range $0 < \Omega < R$ it is $\varepsilon_{r1} > 0$, $\varepsilon_{r2} < 0$. The energy of this wave is concentrated on the top surface of the plasma or it is guided along the plasma-air interface toward positive $\hat{z}$. In contrary, the waves propagating in the negative z-direction behave as $\propto e^{-\kappa_0 \varepsilon_{r2} x / \sqrt{\varepsilon_{r1}}} \cdot e^{+j\kappa_0 \sqrt{\varepsilon_{r1}} \cdot z}$ thus they have their energy concentrated on the lower plasma surface. Hence, they are essentially propagating along the grounded perfect conducting screen. The wave expressions considered before are of the form $e^{\pm \kappa_0 u_p x} \cdot e^{\pm j\kappa_0 \lambda z}$ which can be easily proved that in the limit $\Omega \to 0$ behave just like the above incident waves.

2.10. Wiener-Hopf Formulation of the Shielded Structure

Except the antennas most of other printed microwave structures (e.g., transmission lines) are usually shielded by a metallic plane placed on top and at some distance from the structure. Since the presented approach can be exploited in the characterization of microstrip open-end discontinuities, the next section studies the shielded geometry. The analysis of the latter may serve as the base to extend the method to the open geometry. Besides it may offer valuable insight into the physical phenomena involved through closed form expressions.

The primary reason for studying the shielded geometry is the offered analytical simplicity, since the Kernel $Q(\lambda)$ involved in the resulting wiener-Hopf equation is a meromorphic function. This in turn lends itself to a factorization into a product of closed form "positive" and "negative" spectral functions. Hence, it enables a convenient solution of the Wiener-Hopf equation. In view of these arguments the shielded geometry may serve as a reference solution for the verification of the open geometry presented above. More important, the factorized Kernel of the shielded structure may provide the factorized Kernels of the open geometry by taking the limit where the shield distance tends to infinity. Besides, there is a plethora of microwave devices implemented using shielded printed lines, as explained in the introduction. In turn, their analysis can be understood exploiting the shielded geometry analysis.

The shielded geometry is presented in Fig. 1(b). The general solution of the wave equation and the transverse components in the plasma region are again given by Equations (5) and (7). But in the closed air region $a \le x \le d$ a standing wave solution should be

employed as well:

$$\tilde{H}_y^s = A_p(\lambda)\cosh(\kappa_0 u_0 x) + D_p(\lambda)\sinh(\kappa_0 u_0 x) \quad a \le x \le d \quad (32\text{a})$$

while the transverse components are:

$$\tilde{E}_x^s = -\frac{1}{j\omega\varepsilon_0}\frac{\partial \tilde{H}_y^s}{\partial z} = \zeta_0 \lambda \tilde{H}_y^s \tag{32b}$$

$$\tilde{E}_z^s = \frac{1}{j\omega\varepsilon_0}\frac{\partial \tilde{H}_y^s}{\partial x} = -j\zeta_0 u_0 [A_p(\lambda)\sinh(\kappa_0 u_0 x) + D_p(\lambda)\cosh(\kappa_0 u_0 x)] (32\text{c})$$

The Wiener-Hopf equation is obtained following a procedure similar to that for the open structure. First enforcing the tangential electric field to vanish on the metallic shield at $x = d$ yields:

$$\tilde{E}_z^s(x = d) = 0 \leftrightarrow D_p(\lambda) = -A_p(\lambda)\tanh(\kappa_0 u_0 d) \tag{33a}$$

Using (33a) the field expressions (32a) and (32c) are simplified as:

$$\tilde{H}_y^s(\lambda) = A_p(\lambda)\cdot\frac{\cosh[\kappa_0 u_0(d-x)]}{\cosh(\kappa_0 u_0 d)} \tag{33b}$$

$$\tilde{E}_z^s(\lambda) = +j\zeta_0 u_0 A_p(\lambda)\cdot\frac{\sinh[\kappa_0 u_0(d-x)]}{\cosh(\kappa_0 u_0 d)} \tag{33c}$$

In turn the requirement for the tangential electric field to vanish on the truncated conductor ($x = a$, $z < 0$), similar to Equations (14), yields the definition of a "positive" spectral function as:

$$\tilde{E}_z^s(x = a^+, z < 0) = j\zeta_0 \cdot \tilde{R}_+(\lambda) \tag{34a}$$

where

$$\tilde{R}_+(\lambda) = A_p(\lambda)\cdot u_0 \cdot [\tanh(\kappa_0 u_0 d) - \tanh(\kappa_0 u_0 a)]\cosh(\kappa_0 u_0 a) =$$
$$= A_p(\lambda)\cdot u_0 \cdot \sinh[\kappa_0 u_0(d-a)]/\cosh(\kappa_0 u_0 d) \tag{34b}$$

At the next step the tangential electric field $\tilde{E}_z^s$ is enforced to vanish on the metallic ground plane $x = -a$ and to be continuous at the interface ($x = a$, $-\infty < z < \infty$). The resulting expressions are algebraically manipulated in order to express $B_p(\lambda)$ and $C_p(\lambda)$ in terms of $A_p(\lambda)$ and finally in terms of $\tilde{R}_+(\lambda)$ through (34b) as:

$$A_p(\lambda) = \tilde{R}_+(\lambda)\cdot\cosh(\kappa_0 u_0 d)/[u_0 \cdot \sinh[\kappa_0 u_0(d-a)]] \tag{35a}$$

$$B_p(\lambda) = -\tilde{R}_+(\lambda)\cdot\frac{\varepsilon_{r1}\cdot u_p + \lambda\varepsilon_{r2}\cdot\tanh(\kappa_0 u_p a)}{2(\lambda^2 - \varepsilon_{r1})\cdot\sinh(\kappa_0 u_p a)} \tag{35b}$$

$$C_p(\lambda) = -\tilde{R}_+(\lambda)\cdot\frac{\lambda\varepsilon_{r2} + \varepsilon_{r1}\cdot u_p \cdot\tanh(\kappa_0 u_p a)}{2(\lambda^2 - \varepsilon_{r1})\cdot\sinh(\kappa_0 u_p a)} \tag{35c}$$

Note that the expressions (35b) and (35c) are identical to (15b) and (15c). The difference due to the presence of the shield is absorbed into the definition of $\tilde{R}_+(\lambda)$.

Following the previous section reasoning the boundary condition for the tangential magnetic field leads to expression (20), which must be fulfilled by a "negative" spectral function $\tilde{L}_-(\lambda)$. Substituting for $\tilde{H}_y^s$ from (5a) and (32a) through the spectral coefficients given in (35), the resulting Wiener-Hopf equation reads:

$$Q_c(\lambda)\tilde{R}_+(\lambda) = \tilde{L}_-(\lambda) - \tilde{j}_+^i(\lambda) \tag{36a}$$

where

$$Q_c(\lambda) = \frac{1}{u_0 \cdot \tanh[\kappa_0 u_0(d-a)]} + \frac{\lambda \cdot \varepsilon_{r2} + \varepsilon_{r1} \cdot u_p \cdot \coth(2\kappa_0 u_p a)}{\lambda^2 - \varepsilon_{r1}} \tag{36b}$$

and $\tilde{j}_+^i(\lambda)$ is still given by (18).

2.11. Comparison of Open and Shielded Geometry Kernels

Comparing the Kernels of the open $Q(\lambda)$ and shielded-closed $Q_c(\lambda)$ geometries, given respectively in (22) and (36), their second term is identical. In the limit when the shield distance goes asymptotically to infinity $d \to \infty$ the term $\tanh[\kappa_0 u_0(d - a)] \to 1$ and $Q_c(\lambda)$ reduces to $Q(\lambda)$. Hence, there is only one difference in the denominator of the first term, but this is enough to make $Q_c(\lambda)$ meromorphic. Explicitly, $u_0 = \sqrt{\lambda^2 - 1}$ introduces a pair of branch cuts in the integrals of $Q(\lambda)$ along $u_0 = 0$ or $\lambda = \pm 1$ (note that λ is complex) as shown in Fig. 3(a). In contrary u_p defined in Equation (5b) does not introduce any singularity, since it appears as a function $u_p \coth(pu_p) \to 1/p$ when $u_p \to 0$. Returning to $Q_c(\lambda)$ the u_0 branch cut singularity is transformed to a pole in Equation (36), since:

$$u_0 \tanh(pu_0)|_{u_0 \to 0} \approx pu_0^2\big|_{u_0 \to 0} = p(\lambda^2 - 1)\big|_{\lambda \to \pm 1} \tag{37}$$

where $p = \kappa_0(d - a)$.

Hence, the branch cut singularity of $Q(\lambda)$ is transformed to a pair of poles in the shielded Kernel $Q_c(\lambda)$.

The characteristic equation of the modes propagating beyond the edge at $z = 0$ toward positive-z can be again obtained by setting $Q_c(\lambda) = 0$.

2.12. E-modes of the Shielded Plasma Substrate

As explained in Section 2.8 the eigenmodes of the structure in the absence of the truncated conductor will be of E-mode type. Their characteristic equation is identical to setting $Q_c(\lambda) = 0$, as:

$$
\begin{aligned}
Q_c(\lambda) &= 0 \leftrightarrow u_0 \tanh[\kappa_0 u_0 (d-a)] \cdot [\lambda \varepsilon_{r2} + \varepsilon_{r1} \cdot u_p \cdot \coth(2\kappa_0 u_p a)] \\
&\quad + (\lambda^2 - \varepsilon_{r1}) = 0
\end{aligned}
\tag{38}
$$

Also the roots of (38) are poles of the Kernel $Q_{ce}(\lambda) = 1/Q_c(\lambda)$ to be factorized next.

2.13. Formal Solution of the Wiener-Hopf Equation

For the solution of the Wiener-Hopf equations (21) or (36) they must be separated into "positive" and "negative" terms. In turn the modified Wiener-Hopf technique given by Mittra and Lee [23] will be employed to get analytical expressions for the unknown spectral functions $\tilde{R}_+(\lambda)$ or $\tilde{L}_-(\lambda)$. The key step in this procedure, which usually involves major analytical complexities, is the factorization of the Kernel $Q_e(\lambda)$ into a product of "positive" and "negative" functions. First, (21) and (36) are recast into a more convenient form, as:

$$
Q_e(\lambda) \cdot \tilde{R}_+(\lambda) = \tilde{L}_-(\lambda) - \tilde{j}^i_+(\lambda)
\tag{39}
$$

where $Q_e(\lambda) = \begin{cases} Q(\lambda) & \text{open structure} \\ Q_c(\lambda) & \text{shielded structure} \end{cases}$.

    Recall that for isotropic geometries the Kernel $Q_e(\lambda)$ is an even function of λ resulting into $Q_{e-}(\lambda) = Q_{e+}(-\lambda)$. However, herein the magnetized plasma is anisotropic and this property breaks due to the anisotropy term $(\lambda \varepsilon_{r2})$ occurring in the Kernels (22) and (36b). From a different point of view the anisotropy causes a non-reprocity or equivalently the characteristics of modes propagating in the positive $\hat{z}$ direction are different from those propagating in the negative $\hat{z}$ direction. This causes $Q_{e-}(\lambda) \neq Q_{e+}(-\lambda)$ and makes the factorization non-trivial, as it will be explained next. However, in any case the factorization of the Kernel $Q_e(\lambda)$ reads:

$$
Q_e(\lambda) = Q_{e+}(\lambda) \cdot Q_{e-}(\lambda)
\tag{40}
$$

For a formal solution of (39) one may substitute (40) into (39) to get

$$
Q_{e_+}(\lambda) \cdot \tilde{R}_+(\lambda) = \frac{\tilde{L}_-(\lambda)}{Q_{e_-}(\lambda)} - \frac{\tilde{j}^i_+(\lambda)}{Q_{e_-}(\lambda)}
\tag{41a}
$$

To conclude the separation of (41a), the mixed term of the right hand side must be decomposed into a sum of "positive" and "negative" functions:

$$\frac{\tilde{j}^i_+(\lambda)}{Q_{e_-}(\lambda)} = \tilde{S}_+(\lambda) + \tilde{S}_-(\lambda) \tag{41b}$$

Substituting back yields:

$$\tilde{P}(\lambda) = Q_{e_+}(\lambda) \cdot \tilde{R}_+(\lambda) + \tilde{S}_+(\lambda) = \frac{\tilde{L}_-(\lambda)}{Q_{e_-}(\lambda)} - \tilde{S}_-(\lambda) \tag{41c}$$

Pole singularities are: i) Positive forward $\lambda = \alpha^+_{nf}$, ii) Negative forward $\lambda = -\alpha^-_{nf}$, iii) Positive backward $\lambda = \alpha^+_{nb}$, iv) Negative backward $\lambda = -\alpha^-_{nb}$.

The "positive" term above is regular for $\lambda_i > -\alpha_+$ (Fig. 2), while the "negative" term is regular for $\lambda_i < \alpha_-$. Hence according to Fig. 2, they have a common strip of analyticity in $-\alpha_+ < \lambda_i < \alpha_-$, where they should be equal to an entire function $\tilde{P}(\lambda)$. According to Liouville's theorem $\tilde{P}(\lambda)$ must be a polynomial or a constant and this behavior is determined by the edge condition in electromagnetic problems. Note that for the present problem the width of this analyticity strip is defined by the minimum losses of the two media: plasma and air. Thus, small losses are formally assumed for the air media as $\text{Im}(\kappa_0) = \alpha_- = \alpha_+$ and the lossless solution is recovered by taking the limit of the losses tending to zero.

Let us now proceed with the factorization of the Kernel for the shielded structure.

2.14. Factorization of the Shielded Geometry Meromorphic Kernel

The Kernel $Q_e(\lambda)$ of the shielded geometry is a meromorphic function. Hence, it can be in principle factorized based on its zeros and poles according to Noble [22] or Mittra and Lee [23]. The expressions obtained are formally similar to those of Janaswamy [24], who studied asymmetric slotlines printed on isotropic substrate. However, in the present case due to the plasma anisotropy the Kernel is not an even function as usually when reciprocal isotropic material is involved. Hence, the factorization of the Kernel is not trivial and the original factorization concept must be reconsidered. According to Noble [22, p.40] and the original reference Titchmarsh [30, p.114] a meromorphic function $f(\lambda)$ which has simple zeros at $\lambda = \alpha_n$, $n = 0$,
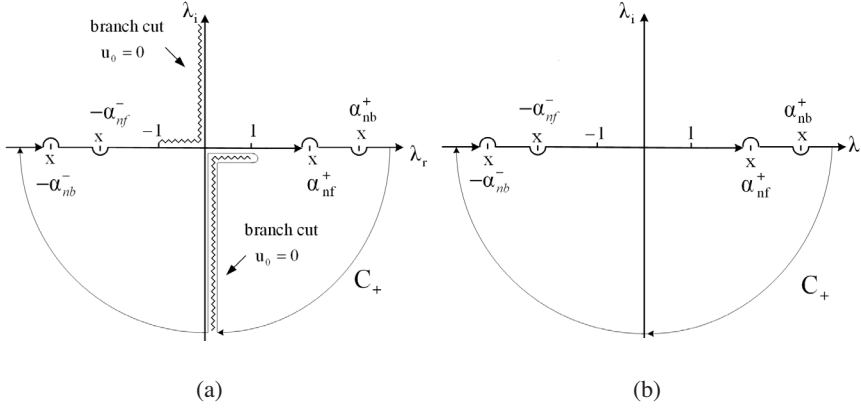
Figure 3. Singularities and integration path for the inversion of (a) open and (b) shielded geometry.

1, 2, ..., ∞ which asymptotically behave as $\alpha_n = \alpha_\infty = \alpha' \cdot n + \alpha''$ can be expanded into an infinite product:

$$f(\lambda) = f(0) \cdot \exp\left[\lambda \cdot f'(0)/f(0)\right] \cdot \prod_{n=1}^{\infty} (1 - \lambda/\alpha_n) \cdot e^{\lambda/\alpha_n} \qquad (42)$$

In the usual case when $f(\lambda)$ is an even function its roots occur in pairs $\lambda = \pm\alpha_n$ and its factorization is given in [22, 23]. The basic idea for the factorization refers to which zeros occur in the upper and respectively lower λ half-planes. This becomes clear when the material losses are considered as: $\varepsilon_r \rightarrow \varepsilon_r^* = \varepsilon_r' - j\varepsilon_r'' = \varepsilon_r'(1 - j\tan\delta)$. Since the wavenumbers and the zeros in turn are proportional to $\pm\sqrt{\varepsilon_r}$, those with a positive real and negative imaginary parts are shifted below the real λ-axis, while those with a negative real part have positive imaginary part and are shifted upwards above the real λ axis. However, this shift is only true for forward surface wave modes where the phase (v_p) and group (v_g) velocities have the same sign. But it was noted in Section 2.9 that in the open structure (Fig. 1(a)) backward surface wave modes with oppositely directed $\vec{v}_p$ and $\vec{v}_g$ occur as well, see also [26]. Since, the surface wave energy is concentrated on the plasma-air interface, thus the same wave properties are expected for the shielded geometry (Fig. 1(b)). A detailed study of the characteristic Equation (38) reveals the same phenomena as those observed in (30). An important question arising at this point is whether poles corresponding to forward and backward modes are shifted toward the same λ-half plane when losses are included. The answer has already

been given by Tamir and Oliner [37, p.321], who elaborated on isotropic plasma layer and with a time dependence $e^{-j\omega t}$. Let us examine this phenomenon following [37]. For this purpose a small loss term $\Delta\kappa = -j\Delta\kappa_0$ can be added to the air wavenumber $\kappa_0 = \omega/c \rightarrow \kappa_0 + \Delta\kappa$, which can be set to zero ($\Delta\kappa \rightarrow 0$) in a limiting process to obtain the ideal lossless case. In turn, the propagation constant along the z-axis defined as $\beta = \kappa_0 \lambda$ will be shifted by an imaginary amount $\Delta\beta$ as:

$$\Delta\beta = \frac{\partial\beta}{\partial\kappa_0} \cdot \Delta\kappa = \frac{\partial\beta}{\partial\omega} \cdot \frac{\partial\omega}{\partial\kappa_0} \cdot \Delta\kappa = \frac{\partial\beta}{\partial\omega} \cdot \frac{\omega}{\kappa_0} \cdot \frac{\beta}{\beta} \cdot \Delta\kappa$$

or

$$\frac{\Delta\beta}{\beta} = \frac{\partial\beta}{\partial\omega} \cdot \frac{\omega}{\beta} \cdot \frac{\Delta\kappa}{\kappa_0} = \frac{\upsilon_p}{\upsilon_g} \cdot \frac{(-j\Delta\kappa_0)}{\kappa_0}.$$

From the above is obvious that forward-positive modes present a negative imaginary shift $\Delta\beta \propto (-j\Delta\kappa_0)$ or toward the negative λ-half plane. In contrary backward modes have $\upsilon_p/\upsilon_g < 0$, thus when they are positive the present $\Delta\beta \propto (+j\Delta\kappa_0)$ or they are shifted toward the positive λ-half plane. Negative modes behave vice-versa. Namely, "positive forward" zeros $\lambda = \alpha_{nf}^+$ representing propagation toward the positive z-axis, as well as "negative backward" zeros $\lambda = -\alpha_{nb}^-$ propagating toward the negative z-axis, occur in the lower λ half plane. Thus, their infinite product constitutes the "positive" spectral function $f_+(\lambda)$ which is analytic in the upper λ half plane. Likewise, "negative forward" zeros $\lambda = -\alpha_{nf}^-$ as well as "positive backward" zeros $\lambda = \alpha_{nb}^+$ occur in the upper λ half plane and their infinite product constitutes the "negative" spectral function $f_-(\lambda)$ analytic in the lower λ half plane. Notice that these upward-downward shifts occur vice-versa in [37], due to the opposite time dependence considered therein.

Summarizing, the characteristic equation $Q(\lambda) = 0$ is solved and its roots are discriminated into "positive forward" $\lambda = \alpha_{nf}^+$ and "negative backward" $\lambda = -\alpha_{nb}^-$ which are included in the $Q_+(\lambda)$. Similarly "positive backward" $\lambda = \alpha_{nb}^+$ and "negative forward" $\lambda = -\alpha_{nf}^-$ are included in $Q_-(\lambda)$. This procedure yields a factorization $Q(\lambda) = Q_+(\lambda) \cdot Q_-(\lambda)$.

For the even terms of $Q(\lambda)$ their roots occur again in pairs and their factorization is handled in the usual manner. Denoting the poles of the even terms as $\lambda = \pm j b_n$ and $\lambda = \pm j c_n$ with $n = 1, 2, \ldots, \infty$ and presenting an asymptotic behavior as $b_n = b_\infty = b' \cdot n + j b''$, $c_n = c_\infty = c' \cdot n + j c''$ the Kernel $Q(\lambda)$ can be factorized as (this is in

general similar to [22, p.15] and [23, p.91–93]):

$$Q_+(\lambda) \; = \; \sqrt{Q(\lambda=0)} \cdot e^{+X^+(\lambda)} \cdot$$

$$\cdot \frac{\prod\limits_{n=1}^{\infty} (1-\lambda/\alpha_{nf}^+) \cdot e^{j\lambda/\alpha'\cdot n} \cdot \prod\limits_{n=1}^{\infty} (1+\lambda/\alpha_{nb}^-) \cdot e^{j\lambda/\alpha'\cdot n}}{\prod\limits_{n=1}^{\infty} (1+\lambda/jb_n) \cdot e^{j\lambda/b'\cdot n} \cdot \prod\limits_{n=1}^{\infty} (1+\lambda/jc_n) \cdot e^{j\lambda/c'\cdot n}} \quad (43)$$

$$Q_-(\lambda) \; = \; \sqrt{Q(\lambda=0)} \cdot e^{-X^-(\lambda)} \cdot$$

$$\cdot \frac{\prod\limits_{n=1}^{\infty} (1+\lambda/\alpha_{nf}^-) \cdot e^{-j\lambda/\alpha'\cdot n} \cdot \prod\limits_{n=1}^{\infty} (1-\lambda/\alpha_{nb}^+) \cdot e^{-j\lambda/\alpha'\cdot n}}{\prod\limits_{n=1}^{\infty} (1-\lambda/jb_n) \cdot e^{-j\lambda/b'\cdot n} \cdot \prod\limits_{n=1}^{\infty} (1-\lambda/jc_n) \cdot e^{-j\lambda/c'\cdot n}} \quad (44)$$

where $X^+(\lambda)$ and $X^-(\lambda)$ are entire functions (without singularities or zeros in the entire λ-plane) which take into account the edge condition at $z = 0$. Thus, to determine $X^\pm(\lambda)$ the edge condition must be invoked. The specific Kernel $Q_c(\lambda)$ of the shielded geometry has the following zeros and poles.

i) Simple zeros at $\lambda = \pm\alpha_n = \mp j\gamma_n$ which are the roots of the characteristic equation $Q_c(\lambda)$ already defined in Equation (38). These can be identified into "positive" and "negative" propagation constants propagating respectively toward the positive and negative z-directions. Besides this each one of them can be characterized either as "forward" or "backward" wave. The corresponding zeros (poles of integrands) shift toward the upper or lower λ half-plane is explained above and it can be summarized as follows:
Poles in the lower λ-half plane:
Positive forward:

$$\lambda = \alpha_{nf}^+ = \alpha_{nrf}^+ - j\alpha_{nif}^+ = -j(\alpha_{nif}^+ + j\alpha_{nrf}^+) = -j\gamma_{nf}^+$$
$$\text{where} \quad \alpha_{nrf}^+, \alpha_{nif}^+ > 0 \qquad\qquad (45a)$$

Negative backward:

$$\lambda = -\alpha_{nb}^- = -\alpha_{nrb}^- - j\alpha_{nib}^- = -j(\alpha_{nib}^- - j\alpha_{nrb}^-) = -j\gamma_{nb}^-$$
$$\text{where} \quad \alpha_{nrb}^-, \alpha_{nib}^- > 0 \qquad\qquad (45b)$$

Poles in the upper λ-half plane:

Positive backward:

$$\lambda = \alpha_{nb}^+ = \alpha_{nrb}^+ + j\alpha_{nib}^+ = j(\alpha_{nib}^+ - j\alpha_{nrb}^+) = +j\gamma_{nb}^+$$
$$\text{where} \quad \alpha_{nrb}^+, \alpha_{nib}^+ > 0 \tag{45c}$$

Negative forward:

$$\lambda = -\alpha_{nf}^- = -\alpha_{nrf}^- + j\alpha_{nif}^- = j(\alpha_{nif}^- + j\alpha_{nrf}^-) = +j\gamma_{nf}^-$$
$$\text{where} \quad \alpha_{nrf}^-, \alpha_{nif}^- > 0 \tag{45d}$$

where α_{nrf}^+, α_{nrf}^-, α_{nrb}^+, α_{nrb}^- are the phase and α_{nif}^+, α_{nif}^-, α_{nib}^+, α_{nib}^- the attenuation constants.

Equations (45a) and (45b) clearly shows that the positive forward zeros $\lambda = \alpha_{nf}^+ = -j\gamma_{nf}^+$ and negative backward $\lambda = -\alpha_{nb}^- = -j\gamma_{nb}^-$ occur in the lower λ-half plane (4th and 3rd quadrants) and should thus constitute the terms of $Q_+(\lambda)$ which is analytical in the upper λ-half plane. Likewise, negative forward zeros $\lambda = -\alpha_{nf}^- = +j\gamma_{nf}^-$ and positive backward $\lambda = \alpha_{nb}^+ = +j\gamma_{nb}^+$ occur in the upper λ-half plane (2nd and 1st quadrants), hence they participate the infinite product of $Q_-(\lambda)$ analytical in the lower λ-half plane. Also, remember that these zeros will be the poles of the integrands in the inverse Fourier transform. The zero order term $-j\gamma_{0f}^+$ and $+j\gamma_{0f}^-$ represent the dominant positive and negative forward propagating modes.

After some algebraic manipulations on (38) its asymptotic behavior for the high order zeros is found as:

$$\alpha_n^+, \alpha_n^- \big|_{n\to\infty} = a_n \big|_{n\to\infty} = \alpha_\infty = a' \cdot n \approx \frac{n\pi}{\kappa_0(d+a)} \tag{46}$$

This is in accordance with that of Janaswamy [24] even though a dielectric rather than a plasma substrate is considered therein.

ii) An infinite number of simple poles at $\lambda = \pm jb_n$ defined by:

$$\sinh[\kappa_0 u_0(d-a)] = 0 \leftrightarrow \kappa_0 u_0(d-a) = jn\pi \tag{47a}$$

or

$$\lambda = \pm jb_n = \pm j\sqrt{\left(\frac{n\pi}{\kappa_0(d-a)}\right)^2 - 1} \tag{47b}$$

The zero order term is $\lambda = \pm jb_0 = \pm j\sqrt{-1} = \mp 1$.
Also, their asymptotic behavior is:

$$b_n\big|_{n\to\infty} = b_\infty = b' \cdot n \approx \frac{n\pi}{\kappa_0(d-a)} \tag{47c}$$

iii) An infinite number of simple poles at $\lambda = \pm jc_n$ defined at:

$$\sinh(2\kappa_0 u_p a) = 0 \leftrightarrow 2\kappa_0 u_p a = jn\pi \qquad (48a)$$

or

$$\lambda = \pm jc_n = \pm j \left\{ \left(\frac{n\pi}{2\kappa_0 a} \right)^2 - \varepsilon_{r_{\mathit{eff}}} \right\}^{1/2} \qquad (48b)$$

The zero order term is $\lambda = \pm jc_0 = \pm j\sqrt{-\varepsilon_{r_{\mathit{eff}}}} = \mp\sqrt{\varepsilon_{r_{\mathit{eff}}}}$.
Likewise, their asymptotic behavior is:

$$c_n|_{n\to\infty} = c_\infty = c' \cdot n \approx \frac{n\pi}{2\kappa_0 a} \qquad (48c)$$

Note that the definition of poles through (47a) and (48a) results from $Q_c(\lambda)$ expression (36b) by writing the tangent and cotangent as ratios of sinus and cosinus functions.

2.15. Edge Condition at $(z = 0,\, x = a)$ Extended along $\hat{y}$

Returning back to the edge condition, it is well understood, e.g., Collin [25, p.25], that the electric and magnetic field components normal to the half plane edge along $\hat{y}$ at $z = 0$ (herein E_x, E_z while $H_x = H_z = 0$) and the related surface charge (ρ_s) as well as the surface current density parallel to the edge (J_{ys}) are singular. For the present problem $J_{ys} = -H_z(x = a)$ is identically zero, as $H_z = 0$. In contrary the field components parallel to the edge (H_y while $E_y = 0$) and the current density normal to the edge (J_{zs}) defined in Equation (23) remain finite tending to zero at the edge. For a metallic half plane placed on top of a dielectric (or just in the air) the singularity behavior is E_x, $E_z \propto (\kappa_0\rho)^{-1/2}$, where $\rho = \sqrt{x^2 + z^2}$ is the distance from the edge extending along $\hat{y}$ at $(z = 0,\, x = a)$. In the Fourier transformed λ-domain, with the aid of Equation (1), this singularity reads, [23, p.13]: $\tilde{E}_x$, $\tilde{E}_z \propto (\kappa_0\lambda)^{-1/2}$. For a prove one may follow [25] which gives for the edge condition

$$\tilde{f}_t(\alpha) \approx A\Gamma(p + 1)(-j\alpha)^{-(p+1)} \quad \text{as} \quad |\alpha| \to \infty \qquad (49a)$$

The two singular components of the present case for the edge at $z = 0$ and $p = -1/2$ yield

$$\tilde{E}_x, \tilde{E}_z \propto A \cdot \Gamma(1/2)(-j\kappa_0\lambda)^{-1/2} \qquad (49b)$$

In contrary, the finite quantities H_y and J_{zs} are proportional to $\sqrt{\kappa_0 \rho}$ tending to zero as $\rho \to 0$. The Fourier transform (1) of this dependence yields $\tilde{H}_y^s, \tilde{j}_-^s \propto (\kappa_0 \lambda)^{-3/2}$. The latter is in accordance with the behavior $(-j\kappa_0 \lambda)^{-(p+1)}\big|_{p=+1/2}$ defined in [23, p.13] for non-singular (vanishing) field components at the edge.

In view of the above edge condition requirements the factorized Kernel $Q_+(\lambda)$ must have an algebraic behavior $Q_+(\lambda) \propto (\kappa_0 \lambda)^{-1/2}$ as $|\lambda| \to \infty$. Likewise, $Q_-(\lambda)$ must present the same algebraic behavior $Q_-(\lambda) \propto (\kappa_0 \lambda)^{-1/2}$ as $|\lambda| \to \infty$. Hence $X^+(\lambda)$ and $X^-(\lambda)$ in Equations (43) and (44) should be defined so that the total argument of the exponential functions involved in the corresponding asymptotic $|\lambda| \to \infty$ expressions vanishes. In order to derive this asymptotic formula we make use of an infinite product identity, [23, p.13]:

$$\prod_{n=1}^{\infty}\left(1+\frac{\lambda}{\alpha \cdot n+b}\right)\cdot e^{-\lambda/\alpha \cdot n} \approx \frac{e^{-\gamma \cdot \lambda/\alpha}\cdot \Gamma(1+b/\alpha)}{\Gamma(1+\lambda/\alpha+b/\alpha)}\bigg|_{b=0} \approx \frac{e^{-\gamma \cdot \lambda/\alpha}}{\Gamma(1+\lambda/\alpha)} \tag{50a}$$

where γ is the Euler's constant.

Equation (50a) can be further simplified by considering the asymptotic approximation of the Gamma function, [31, p.257] or [23, p.14]:

$$\Gamma(\alpha z + b) \approx \sqrt{2\pi}\cdot e^{-\alpha z}\cdot (\alpha z)^{\alpha z+b-1/2} \quad |arg(z)| < \pi, \quad \alpha > 0 \tag{50b}$$

In view of (50b) the asymptotic approximation (50a) is reduced to:

$$\prod_{n=1}^{\infty}\left(1+\frac{\lambda}{\alpha \cdot n}\right)e^{-\lambda/\alpha \cdot n} \approx \left(2\pi \cdot \frac{\lambda}{\alpha}\right)^{-1/2}\cdot \exp\left(-\frac{\lambda}{\alpha}\cdot [\gamma - 1 + \ell n(\lambda/\alpha)]\right) \tag{50c}$$

where the identity $z^z = (e^{\ell n z})^z = e^{z \ell n z}$ is used.

Exploiting (50) in (43) and (44) using also the asymptotic values of zeros and poles, the asymptotic approximations $|\lambda| \to \infty$ of the two factorized Kernels read:

$$Q_+(\lambda)\big|_{|\lambda|\to\infty} \approx \sqrt{Q(\lambda=0)}\cdot e^{+X^+(\lambda)}\cdot \sqrt{2\pi}\cdot \lambda^{-1/2}\left(\frac{\kappa_0(d+a)}{2\kappa_0 a \cdot \kappa_0(d-a)}\right)^{1/2}$$

$$\cdot \exp\left\{-j\frac{\kappa_0 \lambda}{\pi}\cdot [-(d+a)\ell n(d+a) + 2a\ell n(2a)\right.$$

$$\left. +(d-a)\ell n(d-a)]\right\} \tag{51a}$$

$$Q_-(\lambda)\big|_{|\lambda|\to\infty} = Q_+(-\lambda)\big|_{|\lambda|\to\infty} \tag{51b}$$

The anti-symmetry of (51b) is justified by the fact that "positive" and "negative" either forward or backward propagation constants have the same asymptotic expression (46) differing only by a sign. These are in turn obtained by enforcing the total arguments of the exponential functions in (51) to zero:

$$X^-(\lambda) = X^+(-\lambda) \tag{52a}$$

$$X^+(\lambda) = j\frac{\kappa_0\lambda}{2\pi}\cdot[-(d+a)\ell n(d+a)+2a\ell n(2a)+(d-a)\ell n(d-a)] \tag{52b}$$

In view of the above, the asymptotic approximation (51) is reduced to:

$$Q_{c+}(\lambda \to \infty) \approx \sqrt{Q_c(\lambda=0)}.\sqrt{2\pi}\cdot\left(\frac{d+a}{2a(d-a)}\right)^{1/2}\cdot(\kappa_0\lambda)^{-1/2} \tag{53}$$

It is obvious that the above is in accordance with the edge condition. The factorized Kernels in (43) and (44) involves the limiting value at $\lambda=0$:

$$Q_c(\lambda=0) = -\cot[\kappa_0(d-a)] - \sqrt{\varepsilon_{r_{eff}}}\cot\left(2\kappa_0 a\sqrt{\varepsilon_{r_{eff}}}\right) \tag{54}$$

2.16. Final Factorized Kernels

Considering the above analysis the substitution into (43) and (44) yields the final factorized Kernels:

$$
\begin{aligned}
Q_{c+}(\lambda) =\ & \sqrt{Q_c(\lambda=0)}.\frac{\left(1+\lambda/j\gamma_{0f}^+\right)}{(1+\lambda/jb_0)\cdot(1+\lambda/jc_0)} \\
& \cdot\exp\left\{-j\frac{\kappa_0\lambda}{\pi}\cdot[(d+a)\ell n(d+a)-2a\ell n(2a)-(d-a)\ell n(d-a)]\right\} \\
& \cdot\frac{\Gamma(1+\kappa_0\lambda\cdot 2a/j\pi)\cdot\Gamma(1+\kappa_0\lambda\cdot(d-a)/j\pi)}{\Gamma[1+\kappa_0\lambda\cdot(d+a)/j\pi]} \\
& \cdot\prod_{n=1}^{\infty}\frac{(1+\lambda/j\gamma_{nb}^-)}{\Gamma[1+\kappa_0\lambda\cdot(d+a)/jn\pi]}\cdot\prod_{n=1}^{\infty}\left\{\frac{(1+\lambda/j\gamma_{nf}^+)}{\Gamma[1+\kappa_0\lambda\cdot(d+a)/jn\pi]}\right. \\
& \left.\cdot\frac{1+\kappa_0\lambda\cdot(d-a)/jn\pi}{1+\lambda/jb_n}\cdot\frac{1+\kappa_0\lambda\cdot 2a/jn\pi}{1+\lambda/jc_n}\right\}
\end{aligned} \tag{55a}
$$

$$Q_{c-}(\lambda) = \sqrt{Q_c(\lambda = 0)} \cdot \frac{\left(1 - \lambda/j\gamma_{0f}^-\right)}{(1 - \lambda/jb_0) \cdot (1 - \lambda/jc_0)}$$

$$\cdot \exp\left\{+j\frac{\kappa_0\lambda}{\pi} \cdot [(d+a)\ell n(d+a) - 2a\ell n(2a) - (d-a)\ell n(d-a)]\right\}$$

$$\cdot \frac{\Gamma(1 - \kappa_0\lambda \cdot 2a/j\pi) \cdot \Gamma(1 - \kappa_0\lambda \cdot (d-a)/j\pi)}{\Gamma[1 - \kappa_0\lambda \cdot (d+a)/j\pi]}$$

$$\cdot \prod_{n=1}^{\infty} \frac{(1 - \lambda/j\gamma_{nb}^+)}{\Gamma[1 - \kappa_0\lambda \cdot (d+a)/jn\pi]} \cdot \prod_{n=1}^{\infty} \left\{ \frac{(1 - \lambda/j\gamma_{nf}^-)}{\Gamma[1 - \kappa_0\lambda \cdot (d+a)/jn\pi]} \right.$$

$$\left. \cdot \frac{1 - \kappa_0\lambda \cdot (d-a)/jn\pi}{1 - \lambda/jb_n} \cdot \frac{1 - \kappa_0\lambda \cdot 2a/jn\pi}{1 - \lambda/jc_n} \right\} \tag{55b}$$

2.17. Decomposition into Sum of Positive and Negative Functions

The next step in the Wiener-Hopf solution procedure is the decomposition into "positive" and "negative" function terms according to (41b). The only singularity of this equation in the lower λ-half plane is the pole of $\tilde{j}_+^i(\lambda)$ defined in (18) at:

$$\lambda = \sqrt{\varepsilon_{r1}} = [\varepsilon_{r1}'(1 - j\tan\delta)]^{1/2} = n_1' - jn_1'' \tag{56}$$

Observe that when dielectric losses are included, then the pole of Equation (56) is shifted in the lower λ-half plane. Hence, the decomposition is achieved by isolating this pole e.g., [23, p.94]:

$$\frac{\tilde{j}_+^i(\lambda)}{Q_{c-}(\lambda)} = \tilde{S}_-(\lambda) + \tilde{S}_+(\lambda) = \tilde{j}_+^i(\lambda) \cdot \left(\frac{1}{Q_{c-}(\lambda)} - \frac{1}{Q_{c-}(\lambda = \sqrt{\varepsilon_{r1}})} \right)$$

$$+ \tilde{j}_+^i(\lambda) \cdot \frac{1}{Q_{c-}(\lambda = \sqrt{\varepsilon_{r1}})} \tag{57}$$

The above singularity removal approach is actually the same as subtracting and adding the residue contribution at $\lambda = \sqrt{\varepsilon_{r1}}$ (omitting the constant terms).

2.18. Application of Liouvilles Theorem

The last task is the definition of the entire function $\tilde{P}(\lambda)$ in Equation (41c). For this purpose let's consider the asymptotic behavior of each term involved in (39c) as $\lambda \to \infty$. The factorized Kernels $Q_{c-}(\lambda)$ and $Q_{c+}(\lambda)$ behave as $\propto \lambda^{-1/2}$ from (53), while from (18) it

is $\tilde{j}_+^i(\lambda) \propto \lambda^{-1}$. Also, $H_y(z \to 0) \propto z^{1/2}$ as a component parallel to the edge, so $A_p(\lambda) \propto \tilde{H}_y(\lambda) \propto \lambda^{-3/2}$, [23, p.13] and $u_0 \propto \lambda^{+1}$ resulting to $\tilde{R}_+(\lambda) \propto u_0 A_p(\lambda) \propto \lambda^{-1/2}$, which is in accordance with the edge condition of E_z in Equation (33c). Form (57) it is $\tilde{S}_+(\lambda) \propto \lambda^{-1}$ while $\tilde{S}^-(\lambda)$ contains a term $\propto \lambda^{-1/2}$ and one $\propto \lambda^{-1}$. Consequently, all terms involved in (41c) tend to zero as $|\lambda| \to \infty$. Hence, by Liouville's theorem the entire function $\tilde{P}(\lambda)$ is identically zero everywhere, and (41c) yields:

$$\tilde{R}_+(\lambda) = -\frac{\tilde{S}_+(\lambda)}{Q_{c+}(\lambda)} = -\frac{\tilde{j}_+^i(\lambda)}{Q_{c+}(\lambda)} \cdot \frac{1}{Q_{c-}(\lambda = \sqrt{\varepsilon_{r1}})} \tag{58a}$$

$$\tilde{L}_-(\lambda) = \tilde{S}_-(\lambda) \cdot Q_{c-}(\lambda) = \tilde{j}_+^i(\lambda) \cdot \left[1 - \frac{Q_{c-}(\lambda)}{Q_{c-}(\lambda = \sqrt{\varepsilon_{r1}})}\right] \tag{58b}$$

At this point all functions involved in (58) are explicitly known in closed form through (55) and (18). Hence, the spectral functions $\tilde{R}_+(\lambda)$ and $\tilde{L}_-(\lambda)$ are also explicitly defined. Going backwards the spectral coefficients $A_p(\lambda)$, $B_p(\lambda)$ and $C_p(\lambda)$ for the shielded geometry are in turn known through (35) in terms of $\tilde{R}_+(\lambda)$. Likewise, the scattered field components are explicitly defined in the spectral domain through (33b), (32b) and (33c). Besides these, the essentially required expressions are the field quantities in the spatial domain. These can be obtained with the aid of the inverse Fourier transform defined in Equation (2) either in the parallel plane region ($z < 0$), in the grounded plasma area ($z > 0$) as well as in the air region $x > a$. For this shielded geometry the inversion contour of integration is shown in Fig. 3(b). Recall that the involved integrals are meromorphic functions, namely only pole singularities are involved. Thus, the integrals can be conveniently evaluated analytically as a sum of the residue contributions of all poles enclosed within the integration contour. This procedure yields closed form expressions for the field components in the spatial domain. However, this task requires a significant effort since an extensive investigation of the shielded geometry characteristic Equation (38) must be carried out first. This one just like (30) for the grounded slab involves a non-even and non-reciprocal term ($\lambda \varepsilon_{r2}$) resulting from the plasma anisotropy. Hence, similar phenomena to those studied by Seshadri [26] are expected, e.g., non-reciprocal and unidirectional waves. Such a study will include the solution of (38) and its roots constitute the propagation constants. These in turn appear as poles in the integrands which yield the field expression in the spatial domain.

It is clear from the above description that the field evaluation

requires a major effort which may comprise the content of a next article, which will be accompanied by numerical results for specific magnetized solid state plasmas. It is thus logical to conclude this theoretical part at this point.

3. CONCLUSIONS

A geometry of a parallel plane waveguide with a truncated upper conductor and loaded with a magnetized plasma is considered. Wiener-Hopf equations for this structure and the corresponding shielded one are theoretically formulated to characterize the scattering of an extra-ordinary TEM wave normally incident upon the edge of the truncated conductor. Important non-reciprocal and unidirectional wave propagation phenomena are involved as a result of the magnetized plasma anisotropy. Mathematically these phenomena are depicted as non-even Wiener-Hopf Kernels. Hence, their factorization has not been treated in the published literature and new effort is required. Confronting this difficulty the shielded-closed geometry Kernels are factorized yielding the final field expressions. The open geometry Kernel factorization is reserved for a follow up work, to be handled through a limiting approach when the shield distance tends to infinity. Future extensions toward the evaluation of the radiated far field are exceptionally important since novel leaky wave phenomena are expected.

REFERENCES

1. Chen, H., B.-I. Wu, and J. A. Kong, "Review of electromagnetic theory in left-handed materials," *Journal of Electromagn. Waves and Appl.*, Vol. 20, No. 15, 2137–2151, 2006.
2. Mavridis, A. A., G. A. Kyriacou, and J. N. Sahalos, "On the design of patch antennas tuned by transversely magnetized lossy Ferrite including a novel resonating mode," *Progress In Electromagnetics Research*, PIER 62, 165–192, 2006.
3. Ma, Y., V. K. Varadan, and V. V. Varadan, "Prediction of electromagnetic properties of Ferrite composites," *Progress In Electromagnetics Research*, PIER 06, 315–326, 1992.
4. Che, W., E. K. Yung, K. Wu, and X. Nie, "Design investigation on millimeter-wave Ferrite phase shifter in substrate integrated waveguide," *Progress In Electromagnetics Research*, PIER 45, 263–275, 2004.
5. Matsunaga, M., "A coupled-mode theory-based analysis of

coupled microstrip lines on a Ferrite substrate," *Progress In Electromagnetics Research*, PIER 42, 219–232, 2003.

6. Zagriadski, S. V. and S. Choi, "Excitation and reception of electromagnetic, magnetostatic and spin waves in Ferrite films," *Progress In Electromagnetics Research*, PIER 35, 183–216, 2002.

7. Tarkhanyan, R. H. and N. K. Uzunoglu, "Propagation of electromagnetic waves on the lateral surface of a Ferrite/semiconductor superlattice at quantum hall-effect conditions," *Progress In Electromagnetics Research*, PIER 29, 321–335, 2000.

8. Kudrin, A. V., E. Y. Petrov, G. A. Kyriacou, and T. M. Zaboronkova, "Insulated cylindrical antenna in a cold magnetoplasma," *Progress In Electromagnetics Research*, PIER 53, 135–166, 2005.

9. Huang, H., Y. Fan, B.-I. Wu, F. M. Kong, and J. A. Kong, "Surface modes at the interfaces between isotropic media and uniaxial plasma," *Progress In Electromagnetics Research*, PIER 76, 1–14, 2007.

10. Jandieri, G. V., A. Ishimaru, V. G. Jandieri, A. G. Khantadze, and Z. M. Diasamidze, "Model computations of angular power spectra for anisotropic absorptive turbulent magnetized plasma," *Progress In Electromagnetics Research*, PIER 70, 307–328, 2007.

11. Qian, Z. H., R. Chen, K. W. Leung, and H. W. Yang, "FDTD analysis of microstrip patch antenna covered by plasma sheath," *Progress In Electromagnetics Research*, PIER 52, 173–183, 2005.

12. Soliman, E. A., A. Helaly, and A. A. Megahed, "Propagation of electromagnetic waves in planar bounded plasma region," *Progress In Electromagnetics Research*, PIER 67, 25–37, 2007.

13. Hunsberger, F., R. Luebbers, and K. Kunz, "Finite-Difference Time-Domain analysis of gyrotropic media-I: Magnetized plasma," *IEEE Trans. Antennas and Propagation*, Vol. 40, 1489–1495, Dec. 1992.

14. Kashiwa, T., N. Yoshida, and I. Fukai, "Transient analysis of a magnetized plasma in three-dimensional space," *IEEE Trans. Antennas and Propagation*, Vol. 36, 1096–1105, Aug. 1988.

15. Kashiwa, T., N. Yoshida, and I. Fukai, "Time domain analysis of patch antennas in a magnetized plasma by a spatial network method," *IEEE Trans. Antennas and Propagation*, Vol. 39, 147–150, Feb. 1991.

16. El-Sherbiny, A. M., "Hybrid mode analysis of microstrip lines on anisotropic substrates," *IEEE Trans. Microwave Theory Tech.*, Vol. 29, 1261–1265, Dec. 1981.

17. El-Sherbiny, A. M., "Exact analysis of shielded microstrip lines and bilateral fin lines," *IEEE Trans. Microwave Theory Tech.*, Vol. 29, 669–675, July 1981.

18. Kyriacou, G. A. and J. N. Sahalos, "The edge admittance model for the study of microstrips on uniaxial substrate," *Archiv. für Elektrotech.*, Vol. 76, 169–179, 1993.

19. Kyriacou, G. A. and J. N. Sahalos, "A Wiener-Hopf type analysis of microstrips printed on uniaxial substrates: Effect of the substrate thickness," *IEEE Trans. Microwave Theory Tech.*, Vol. 43, 1967–1977, Aug. 1995.

20. Kyriacou, G. A. and J. N. Sahalos, "A Wiener-Hopf type analysis of uniaxial substrates-superstrate microstrip structures," *IEEE Trans. Microwave Theory Tech.*, Vol. 45, 616–629, May 1997.

21. Johansen, E. L., "The radiation properties of a parallel-plane waveguide in a transversely magnetized homogeneous plasma," *IEEE Trans. Microwave Theory Tech.*, Vol. 13, 77–89, Jan. 1965.

22. Noble, B., *Methods Based on the Wiener-Hopf Technique*, Pergamon Press, 1958.

23. Mittra, R. and S. W. Lee, *Analytical Techniques in the Theory of Guided Waves*, McMillan, New York, 1971.

24. Janaswamy, R., "Wiener-Hopf analysis of the asymmetric slotline," *Radio Science*, Vol. 25, No. 5, 699–706, 1990.

25. Collin, R. E., *Field Theory of Guided Waves*, 2nd edition, IEEE Press, NJ, 1990.

26. Seshadri, S. R. and W. F. Pickard, "Surface waves on an anisotropic plasma sheath," *IEEE Trans. Microwave Theory and Techniques*, Vol. 12, 529–541, Sept. 1964.

27. Kobayashi, K., S. Koshikawa, and A. Sawai, "Diffraction by a parallel-plate waveguide cavity with dielectric/Ferrite loading: Part I - The case of E polarization," *Progress In Electromagnetics Research*, PIER 08, 377–426, 1994.

28. Koshikawa, S. and K. Kobayashi, "Diffraction by a parallel-plate waveguide cavity with dielectric/Ferrite loading: Part II - The case of H polarization," *Progress In Electromagnetics Research*, PIER 08, 427–458, 1994.

29. Ishimaru, A., "The effect of the radiation from a plasma sheath of a unidirectional surface wave along a perfectly conducting plane," Techn. Rept., No. 64, College of Engineering, University of Washington, Seattle, April 1962.

30. Titchmarsh, E. C., *The Theory of Functions*, 2nd edition, Oxford University Press, 1939.

31. Abramowitz, M. and I. A. Stegun, *Handbook of Mathematical Functions*, 9th Printing, Dover Publ., 1972.

32. Hoyaux, M. F., "Solid state plasmas," *Applied Physics Series*, Pion Ltd., London, 1970.

33. Talisa, S. H. and D. M. Bolle, "Performance predictions for isolators and differential phase shifters for the near-millimeter wave range," *IEEE Trans. on Microwave Theory and Tech.*, Vol. 29, 1338–1343, Dec. 1981.

34. Hwang, W. L. and D. M. Bolle, "Magnetoplasma surface wave analysis for an H-guide structure containing semiconductor," *Int. J. Infrared & Mil. Waves*, Vol. 4, No. 5, 819–830, 1983.

35. Ivanov, S. T. and N. I. Nikolaev, "Magnetic-field effect on wave dispersion in a free semiconductor slab," *J. Phys. D: Appl. Phys.*, Vol. 32, 430–439, 1999.

36. Mittra, R. and S. W. Lee, "Mode Matching Method for anisotropic guides," *Radio Science*, Vol. 2, No. 8, 937–942, 1967.

37. Tamir, T. and A. A. Oliner, "The spectrum of electromagnetic waves guided by a plasma layer," *IEEE Proc.*, Vol. 51, 317–332, Feb. 1963.

38. Barybin, A. A., "Modal expansions and orthogonal complements in the theory of complex media waveguide excitation by external sources for isotropic, anisotropic, and bianisotropic media," *Progress In Electromagnetics Research*, PIER 19, 241–300, 1998.